IN-SITU ALLOYING OF TI6AL4V-x%CU STRUCTURES BY DIRECT METAL LASER SINTERING

E.B. Newby[1]*, D. Kouprianoff[1], I. Yadroitsava[1]

[1]* Department of Mechanical and Mechatronic Engineering
Central University of Technology, South Africa
(Corresponding author: ericnewby1@hotmail.com)

ABSTRACT

The formation of in-situ Ti6Al4V-x%Cu (1%, 3% and 5% Cu) alloy structures by Direct Metal Laser Sintering (DMLS) for application in medical implants was investigated. Ti6Al4V (ELI) powder was mixed with pure Cu powder of similar particle size distribution. Optimal process parameters were established for in-situ alloying of Ti6Al4V-x%Cu to form dense parts with suitable microstructural and surface quality. Process parameters such as laser power, scanning speed, hatch distance and layer thickness directly affect the surface quality and part density. Firstly, single track formation was studied at different scanning speeds for 170 W and 340 W laser powers. The effect of laser power and scanning speed on the track width and shape was described. Secondly, the surface roughness and single layer morphology were considered.

1. INTRODUCTION

Ti6Al4V Extra Low Interstitial (ELI) alloy is commonly used for medical implants because of its biocompatibility and suitable mechanical- and corrosion resistant properties. The most common reason for implant failure and complication after surgery, is infection. Manufacturing implants from materials with antibacterial properties (such as Cu) is a promising approach to infection prevention [1, 2]. Copper is a proven antibacterial agent and in small amounts not toxic to the human body [1]. DMLS can be applied to directly produce implants having a biocompatible Ti6Al4V structure with Cu additions at the bone–implant interface to reduce the risk of bacterial infection and implant failure.

Fundamentally, DMLS is an Additive Manufacturing (AM) process in which a laser beam is scanned over a thin powder layer. The laser beam melts a row of powder particles, forming a molten pool and finally a single track. Single tracks, or the continuous linear formation of the molten pool is the most basic building block in the DMLS process. DMLS objects are formed by fusing multiple single tracks layer by layer upon one another. Thus the optimization of formation of the molten pool and single track plays a major role in the quality and mechanical properties of the manufactured 3D object [3].

The geometric characteristics of the DMLS tracks are mainly determined by material properties, energy input (laser power, spot size and scanning speed) and the thickness of the deposited powder layer. The depth of penetration into the substrate is determined primarily by the power of the laser beam, and the layer thickness which determines the powder volume involved in the melting process [3, 4]. At optimal process parameters, DMLS single tracks are continuous and have stable geometrical characteristics.

Single tracks produced with DMLS can be characterised into continuous tracks with regular geometrical characteristics (Figure 1, zone B) and undesired irregular tracks (Figure 1, zones A and C). Single track formation is directly influenced by the process parameters. If the scanning speed decreases, it results in a higher linear energy input (power per unit speed). Irregular tracks in zone A; are formed at higher energy inputs and the heat affected zone becomes larger involving more powder particles. Tracks in zone A tend to have more satellites or dislodged sections that form during solidification. Deep keyhole penetration into the substrate and surface-satellites provoke porosity in the final 3D part. Drop formation (balling effect) occurs at insufficient energy input because the surface tension breaks the melting single track into individual droplets (zone C). At low effective power the powder experiences lower temperatures, thus the surface tension coefficient as well as melt viscosity increase leading to drop formation [5].

Modern DMLS systems use fibre lasers with high power densities. For a laser power of 200 W and a spot size of 80 μm, power density reaches ~40 kW/mm^2. The concentrated heat input of the DMLS process leads to high thermal gradients which induce residual stress within the part. After laser scanning, the stress state near the surface of the part is biaxial and in tension, the major component is double that of the minor stress [6]. High residual stress leads to part deformation, delamination from the substrate during manufacturing and crack propagation. Cracks in the DMLS parts are indicates that the ultimate tensile strength of the material has been exceeded during manufacturing.

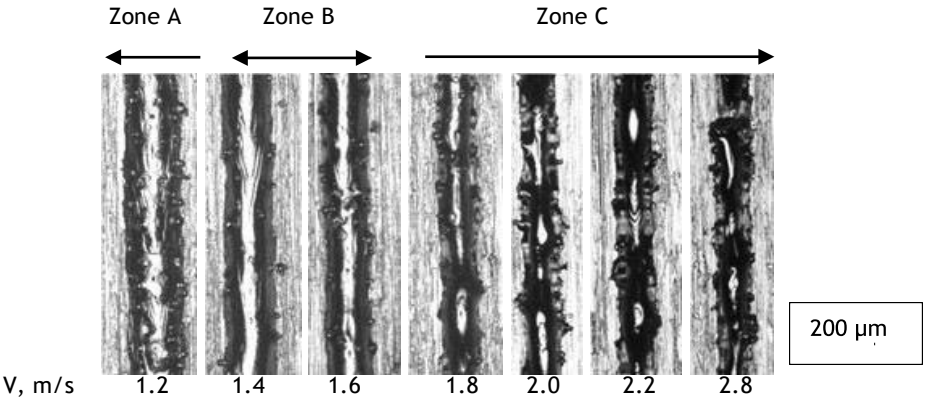

Figure 1: Ti6Al4V tracks at the substrate at 300 W laser power and different scanning speeds

This research was aimed at obtaining an insight into the development of the single-track and layer formation of Ti6Al4V-x%Cu (1at.%, 3at.% and 5at.% Cu) during DMLS. Since single layer is a superposition of the synthesized single tracks, surface morphology of the layers depends on geometrical characteristics of single tracks, scanning strategy and hatch distance. Roughness of the sintered single layer defines the thickness and homogeneity of the next layer. Non-uniform thickness of the next deposited powder layer could be critical for the resulting part. If the deposited powder layer is too thick for a set of chosen process-parameters the penetration depth will not be great enough for it to fuse into the previous layer, pores will occur in the DMLS

sample. The influence on track geometry and morphology of the layers of different scanning speeds, laser power and %Cu were investigated in this work.

2. METHODOLOGY

Argon atomized Ti6Al4V (ELI) and Cu powder spherical in shape were used. Chemical composition for Ti6Al4V (ELI) being 89.26 wt% of Ti, 6.31 wt% of Al, 4.09 wt% of V, 0.12% of O, and Cu powder 99.9 % purity. Thermo-physical properties of employed materials are shown in Table 1. The 10th, 50th and 90th percentiles of equivalent diameter (weighted by volume) were respectively 12.6 µm, 22.9 µm, 37.0 µm for Ti6Al4V (ELI) powder and 9.45 µm, 21.9 µm and 37.5 µm for Cu powder. To produce the Ti6Al4V-x at.%Cu powder mixture, the elemental Cu and Ti6Al4V(ELI) powders were mixed for 1 hour. Before laser processing, the powders mixture was dried at 80°C for 2 hours without protective atmosphere, to increase powder flow ability.

Table 1. Thermo-physical properties of employed materials

	Ti6Al4V	Cu
Specific heat capacity, J/(kg×K)	560	387
Thermal conductivity, W/(m×K)	7.2	401
Thermal diffusivity, m^2/s	2.9×10^{-6}	1.16×10^{-4}
Density, kg/m^3	4430	8940
Melting temperature, K	1922	1356
Latent heat of fusion, kJ/kg	370	205
Viscosity in liquid state, mPa×s		
1356 K		4.02 [8]
1950 K		1.96 [8]
1750-2050 K	4.42 [7]	

To determine the effect of scanning speed and laser power as well the influence of amount Cu on the DMLS process, single tracks with length of 20 mm and surfaces with size 10 mm x 5 mm were manufactured by an EOSINT M280 machine. Three tracks were produced at each set of process parameters. Two sets of process parameters were used: laser power 170 W at six scanning speeds (0.4 m/s, 0.6 m/s, 0.8 m/s, 1 m/s, 1.2 m/s and 1.4 m/s) and laser power 340 W at increase in scanning speeds by two times accordingly. Laser spot size was approximately 80 µm and the powder layer thickness was 50 µm. This strategy was then carried out on all three Ti6Al4V-x%Cu alloys (1at%, 3at% and 5at%).
The building chamber was filled with an inert (Argon) atmosphere. This results in an atmosphere with a low oxygen content during building. Experiments were done on Ti6Al4V substrates with 3 mm thickness which was attached to the machine base plate with 4 screws in the corners.

3. RESULTS AND DISCUSSION

To determine the influence of the process parameters in the formation of the single-tracks, two different laser powers were used at different scanning speeds. In the first set, the laser power was set at 170 W for each scanning speed, applied to the Ti6Al4V-x%Cu powder mixtures and then a similar set was done at 340 W laser power at double the scanning speed.

At 170 W laser power and 1%Cu, balling effect was found only at 1.8 m/s and higher, for 3%Cu the balling effect starts to be noticed at a scanning speed of 1.2 m/s. The surface tension deformed the track though the track is still continuous at these scanning speeds (Figure 2). For scanning speeds lower than 1.0 m/s the tracks are fully continuous and stable with no signs of irregularity. At 5%Cu, DMLS tracks were regular and continuous up to 1.4 m/s.
Figure 3 shows single tracks at 340 W laser power. As predicted, drop formation becomes less with the increase in laser power; the range of scanning speeds where tracks were continuous increased with laser power. With an increase in scanning speed the single track width decreased (Figure 4). Also track's width at lower laser power (170 W) had a tendency to be wider with an increase of copper in the initial powder mixture. This can be a result of slight variation in powder layer thickness for the experiments but also due to more prominent capillary flow effect in the molten pool with higher copper content. At the temperature close to melting point of Ti6A4V, copper has very low viscosity (Table 1) and wetting dynamics can be different in comparison with lower percent of Cu in powder mixture. Changes in thermo-physical properties of the material may also be a reason for this phenomena.

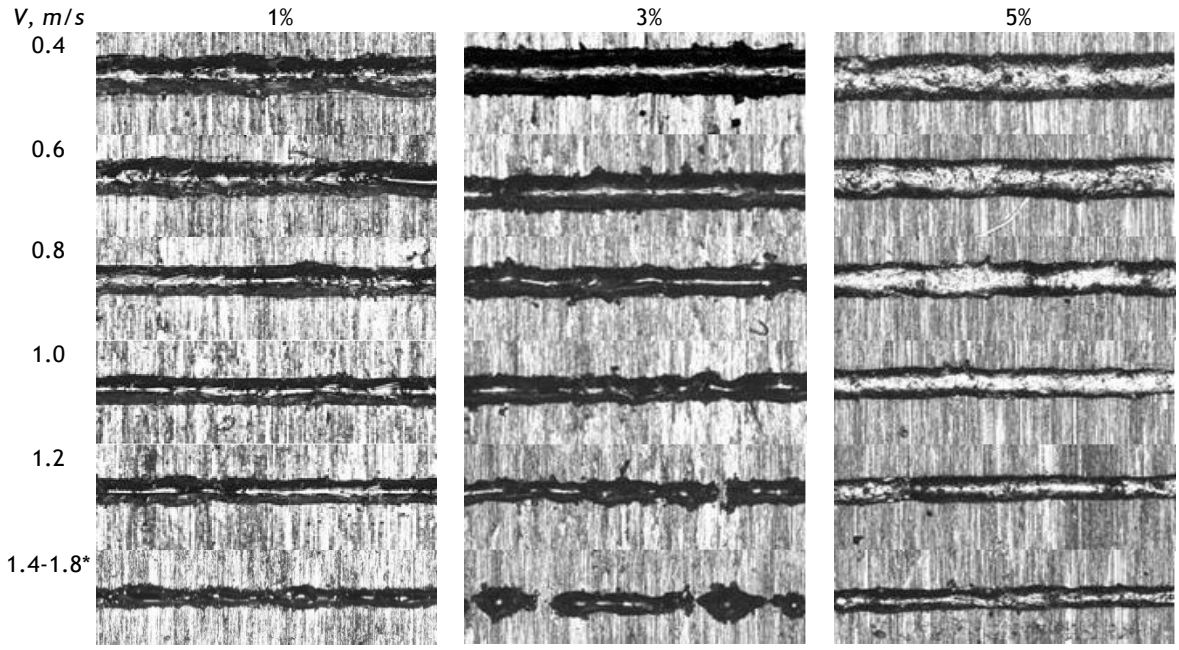

* For 1at%Cu, scanning speed was 1.8 m/s, for 3-5at.%Cu it was 1.4 m/s

Figure 2: Single tracks at 170 W laser power at different scanning speeds

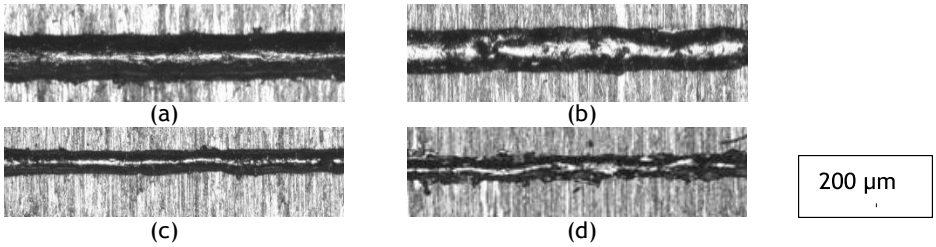

Figure 3: Single tracks at 340 W laser power at scanning speeds: (a, b) 0.8 m/s and (c, d) 2.8 m/s for 3% (a, c) and 5%Cu (b, d)

At the higher laser power (340 W) the difference between 3% and 5% track width was negligible, but tracks were about 30% wider compared to 170 W. Higher laser power density led to a higher temperature in the molten pool and accelerated fluid flow.

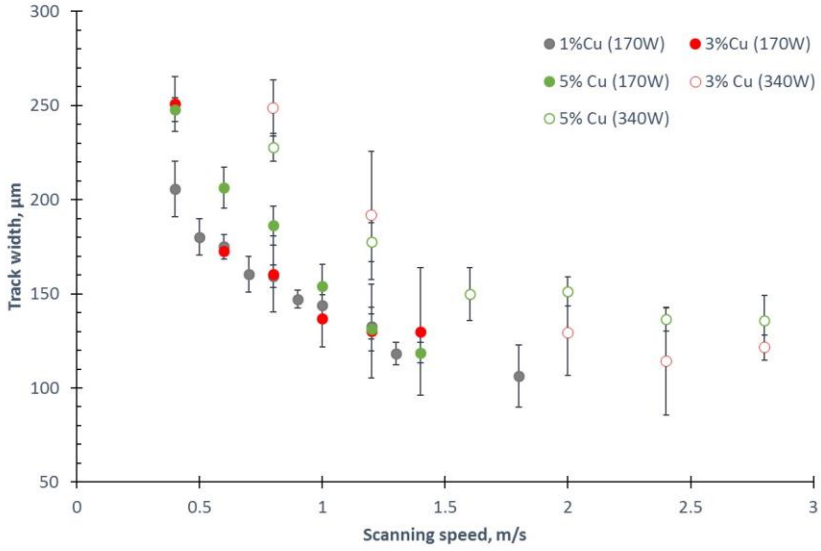

Figure 4: Single tracks at various scanning speeds for Ti6Al4V- *x*at.% Cu

On the top surface of the tracks, cracks were found at 3 and 5 at.% of Cu (Figure 5). When the powder mixture is exposed to the laser beam, it melts, but since Cu has a higher thermal conductivity and lower heat capacity than Ti6Al4V (Table 1), copper transfers heat to the surrounding titanium alloy faster. Different properties of powder materials influence the in-situ alloying and the resulting DMLS material properties. Ti6Al4V has a higher melting point and absorbs more energy from the laser beam than Cu.

In pilot study [9] was shown that at 170 W laser power, 0.7 m/s scanning speed, 80 μm hatch distance and 30 μm layer thickness, 3D samples of Ti6Al4V-1at.%Cu were inhomogeneous and had Cu-enriched regions. In [10] the presence of hard intermetallic compounds in DMLS Ti6Al4V-xCu alloys was found. The relative diffraction intensity of Ti_2Cu phase gradually increased with the Cu contents. This may have an influence on mechanical properties. High residual stress during DMLS and embrittlement of the material with intermetallics led to crack creation. This effect became more pronounced with an increase in copper content in the initial powder mixture (Figure 5).

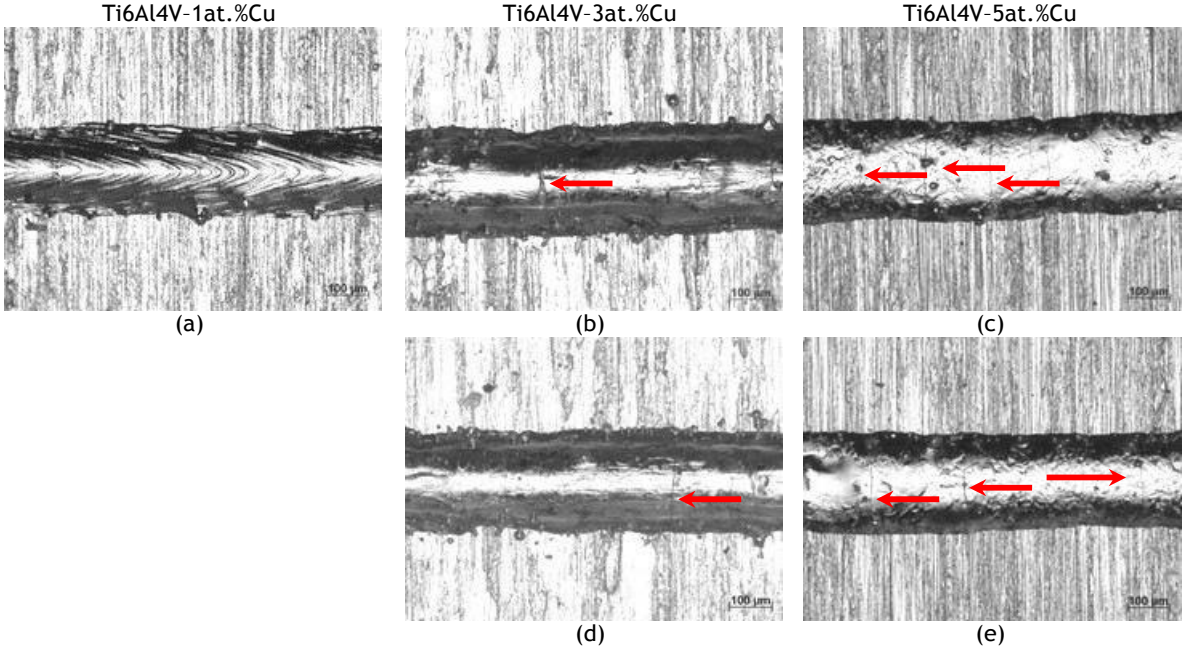

Figure 5: Single tracks at 170 W laser power at 0.4 m/s scanning speed (a-c) and 350 W and 0.8 m/s (d-e)

The second set of data shows surfaces at 170 W laser power with a scanning speed of 0.4-1.4 m/s, 340 W laser power and scanning speeds of 0.8-2.8 m/s and hatch distance of 80 μm. On 1%Cu samples, solidification lines and grain boundaries were clearly visible (Figure 6). As it was indicated, experiments were done on a 3 mm plate attached to the base plate with 4 screws in the corners. After detaching the substrate from the base plate, the thin substrates deformed due to introduced residual stresses during DMLS processing. Cracks across tracks, perpendicular to the scanning direction were found on the 3% and 5% Cu layers, but not in the first experiment with Ti6Al4V-1 at.%Cu samples (Figure 6 and Figure 7).

It was shown previously that in DMLS Ti6Al4V samples near the surface, major principal stress was parallel to the scanning direction [6]. In the present study, cracks perpendicular to the scanning direction were found in single tracks (Figure 5 b-e) and single layers (Figure 6 c-f and Figure 7b-c). After formation of cracks perpendicular to the scanning direction, relaxation of the major component of residual stress occurred, shear and minor stresses became dominant. If these stresses were higher than the ultimate tensile strength of the sintered material, other directional cracks would form.

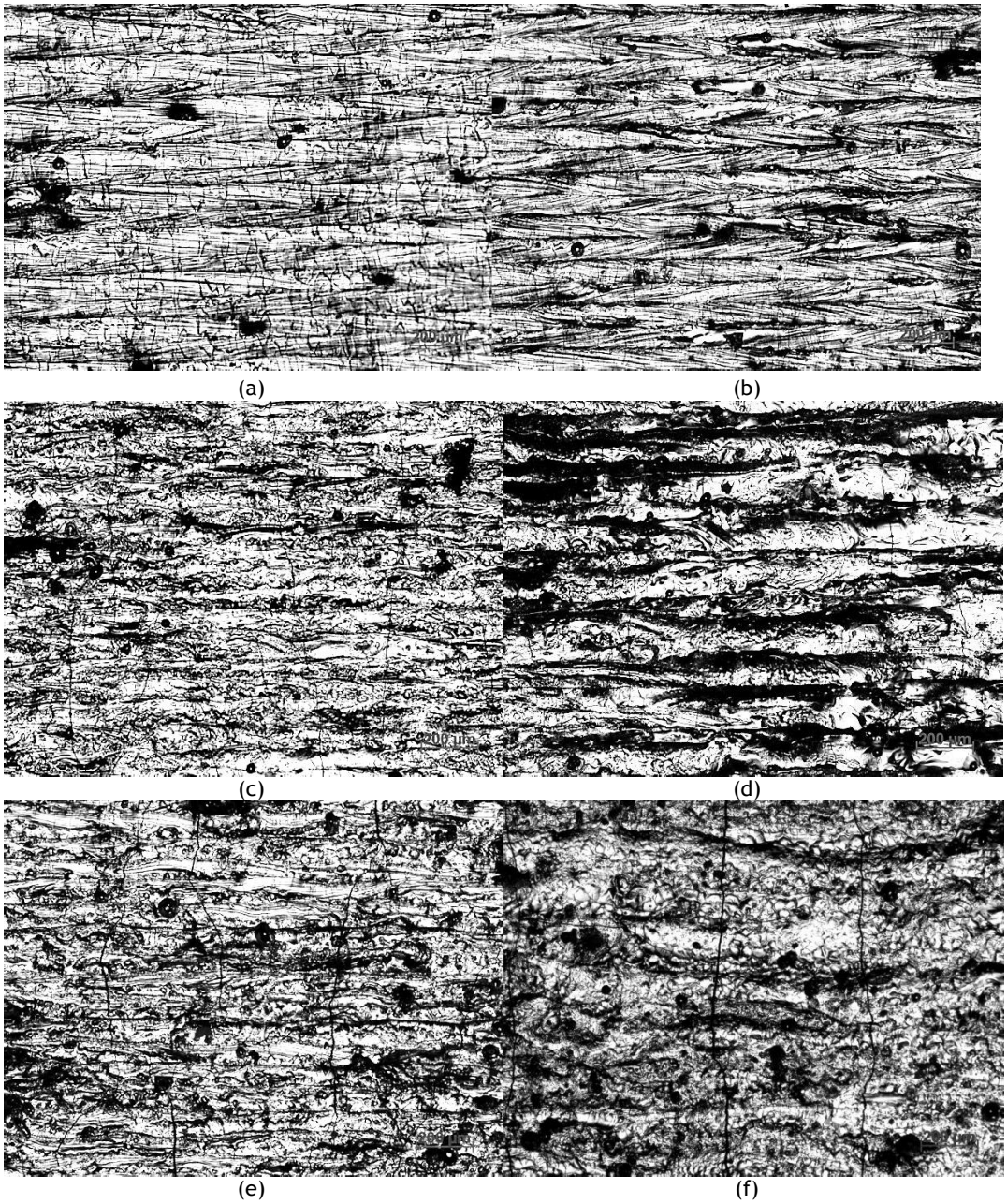

Figure 6: Single layers at 170 W and 0.6 (a), 1.3 m/s (b) in 1%Cu samples; 170 W, 0.6 m/s (c) and 340 W, 1.4 m/s (d) in 3%Cu samples; 170 W and 0.6 m/s (e), and 340 W, 1.2 m/s (f) in 5%Cu samples at hatch distance of 80 µm

In produced samples, transversal cracks were dominated in 3–5at.% in DMLS single layers. The most probable cause of cracks was embrittlement of sintered material with intermetallic phases, further XRD measurements have to be done and analysed for the identification of phases present in the sintered materials. One-scanning direction can lead to deformation of the sample and crack formation in 3D DMLS Ti6Al4V–x%Cu samples, thus changing direction for the next layer to disorientate the residual stress is necessary for producing *in-situ* alloyed samples. Another reason for deeper cracks in Ti6Al4V–5at.% layers can be higher residual stress and lower tensile strength of the *in-situ* alloyed material. Further investigations are required to produce Ti6Al4V– 3-5%Cu alloy by DMLS without cracks.

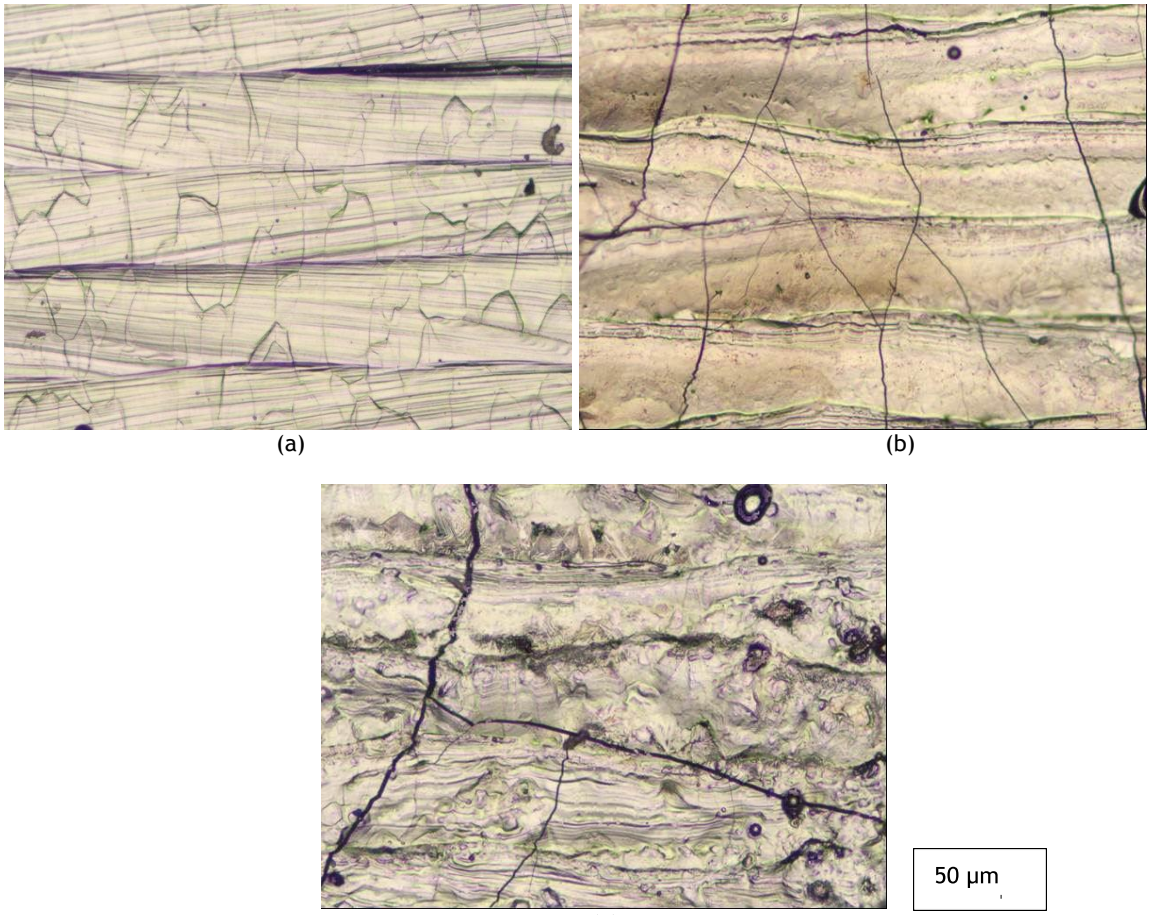

Figure 7: Single layers at 170 W and 0.6 m/s scanning speed after single scan at hatch distance of 80 µm for 1% (a), 3% (b) and 5% Cu (c) samples

The *in-situ* alloyed Ti6Al4V–xat.% DMLS surface morphology showed complex behaviour *when comparing it to* laser power and scanning speed. Surface morphology depends on the shape of the single tracks and the hatch distance. At the hatch distance of 80 µm the surface roughness increased with per cent of Cu and scanning speed (Figure 8a, b). Surfaces at higher scanning speeds produced humping effect and more satellites as the molten pool became more pronounced, especially at higher laser power (Figure 8b). Layer surface quality dramatically decreased at 5%Cu samples with lower energy input (Figure 8c).

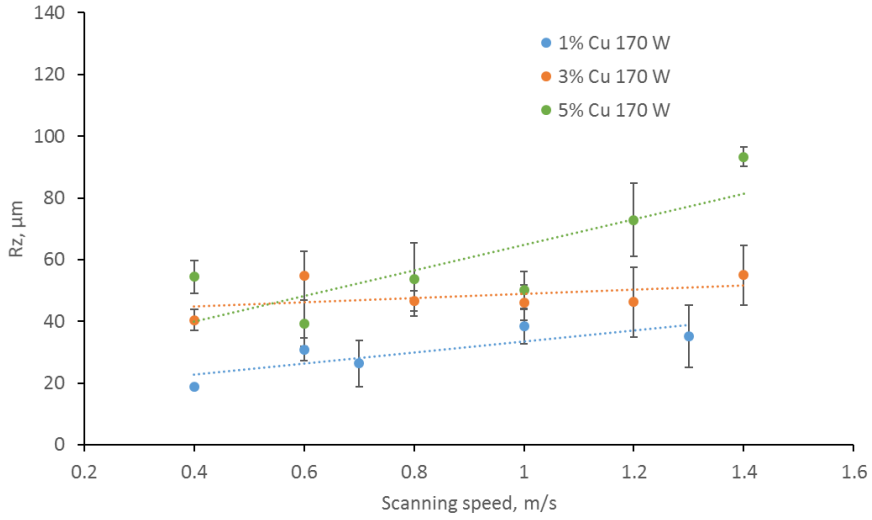

(a)

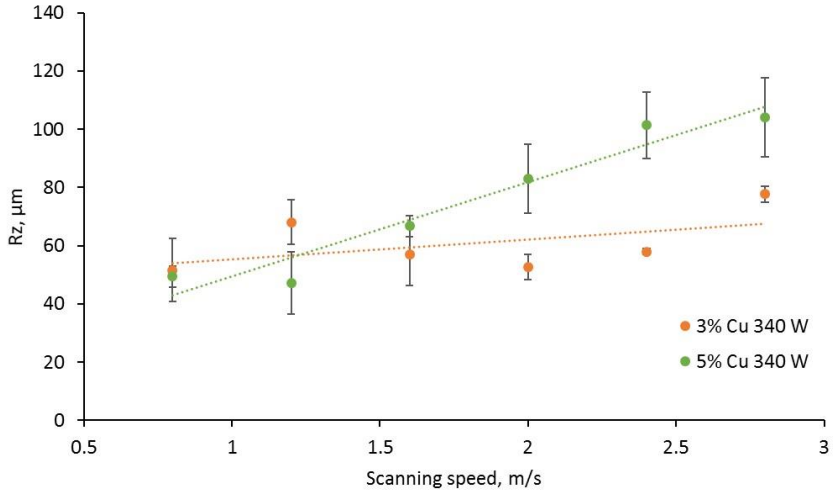

(b)

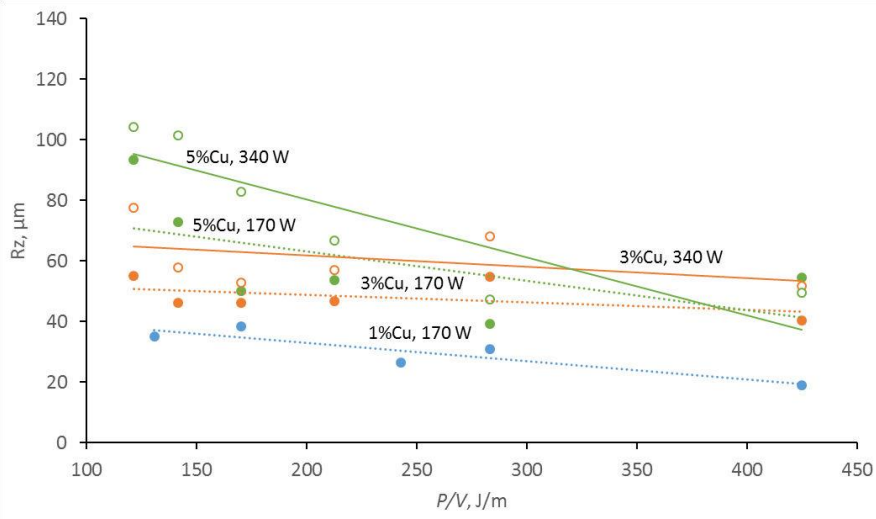

(c)

Figure 8: Surface roughness *Rz* of single layers at 170 W (a), 340W (b) and *versus* energy input (c) at Ti6Al4V-*x*Cu samples at different scanning speeds and hatch distance of 80 µm

4. CONCLUSION

In this work, in-situ alloyed Ti6Al4V-x%Cu single tracks and layers were fabricated. The results indicated that track width increased with laser power, Cu per cent in initial powder mixture and decreasing of scanning speed. The surface roughness of the produced layers improved with a decrease in scanning speed.

From experimental work it was found, that optimal process-parameters for single tracks and single layers are:

- laser power of 170 W, scanning speed ≤1.0 m/s for Ti6Al4V-1-5at.%Cu
- laser power of 340 W, scanning speed about 1.6 m/s for Ti6Al4V-3-5 at%Cu.

The size and number of cracks on the top surface of single layers increased with addition of Cu in initial powder mixture. Cross-sectional analysis will be done to investigate the depth of molten pool and chemical analysis for Cu homogeneity in single layers. The issue of crack formation in Ti6Al4V-3-5 at%Cu requires careful study and elaboration of the procedure to decrease residual stress to avoid crack formation for *in-situ* alloyed 3D DMLS samples.

5. ACKNOWLEDGEMENTS

This work is based on the research supported by the South African Research Chairs Initiative of the Department of Science and Technology and National Research Foundation of South Africa (Grant №97994) and the Collaborative Program in Additive Manufacturing (Contract №CSIR-NLC-CPAM-15-MOA-CUT-01). The authors are grateful to IMCE for carrying out the impulse excitation measurements.

6. REFERENCES

[1] **Liu, R., et al.** 2016. Antibacterial effect of copper-bearing titanium alloy (Ti-Cu) against Streptococcus mutans and Porphyromonas gingivalis. *Scientific Reports* 6, 29985.

[2] **Erinosho, M.F et al.** 2017. Laser surface modification of Ti6Al4V-Cu for improved microhardness and wear resistance properties. Materials Research 20(4), 1143-1152

[3] **Yadroitsev, I., Krakhmalev, P. and Yadroitsava, I.** 2015. Hierarchical design principles of selective laser melting for high quality metallic objects. *Additive Manufacturing*, 7, pp.45-56.

[4] **Vrancken, B., Thijs, L., Kruth, J.P. and Van Humbeeck, J.** 2014. Microstructure and mechanical properties of a novel β titanium metallic composite by selective laser melting. *Acta Materialia*, 68, pp.150-158.

[5] **Yadroitsev, I., Bertrand, P. & Smurov, I.** 2007. Parametric analysis of the selective laser melting process. Applied Surface Science, 253, pp.8064-8069.

[6] **Yadroitsava I., Grewar S., Hattingh D., Yadroitsev I.** 2015. Residual stress in SLM Ti6Al4V alloy specimens, *Materials Science Forum*, 828-829: 305-310.

[7] **Paradis, P.-F., Ishikawa, T., Yoda, S.** 2002. Non-Contact Measurements of Surface Tension and Viscosity of Niobium, Zirconium, and Titanium Using an Electrostatic Levitation Furnace. Int. J. Thermophys. 2002, 23(3), pp. 825–842.

[8] **Assael, M.J., Kalyva, A.E., Antoniadis, K.E., Banish, R.M., Egry, I., Quested, P.N., Wu, J., Kaschnitz, E., Wakeham W.A.** 2010 Reference Data for the Density and Viscosity of Liquid Copper and Liquid Tin. *J. Phys. Chem. Ref. Data*, 39, 033105:1-9.

[9] **Kinnear, A. Dzogbewu, T. C., Krakhmalev, P. Yadroitsava I., Yadroitsev, I.** 2017. Manufacturing, microstructure and mechanical properties of selective laser melted Ti6Al4V-Cu. In: *Lasers in Manufacturing Conference*, Munich, June 26-29, 2017.

[10] **Guo, S., Lu, Y., Wu, S., Liu, L., He, M., Zhao, C., Gan, Y., Lin, J., Luo, J., Xu, X., Lin, J.** 2017. Preliminary study on the corrosion resistance, antibacterial activity and cytotoxicity of selective-laser- melted Ti6Al4V-xCu alloys. *Mater. Sci. Eng.*, C. 2017, 72, 631-640.